Nanoscale Fabrication and Characterization for MEMS Device

Shenshen Wan, Minzhong Gao, University of Pennsylvania

Abstract—**This work focuses on microfabrication technology of fabricating polysilicon electron devices as comb-drive mems devices and cantilever beams. By utilizing a series of techniques including photolithography, deep reactive-ion etching, and HF wet etching processes, eighteen comb-drive mems devices of and ten cantilever beams of different feature sizes were fabricated on one single-crystal silicon chip. The surface morphology, feature size, electrical properties under AC, and DC current were measured. The process of fabrication was improved to make the beams standstill. The error analysis and the next step of processing were also discussed on this page.**

I. Introduction

The electrostatic comb-drives are one of the most common mems actuators. The main advantages of comb-drive are that the fabrication processes are not complex, the dynamic response is fast compared with other mems devices, and the force generated during the motion of the comb is constant[1].

Comb-drive actuators compose of electrostatically connected series of interdigitated combs and beams which can bend and flexed to counteract the electrostatic force. One of the two combs is anchored fixed comb, and the other is a moveable comb which is connected to beams[2]. The comb-drive actuators utilize the electrostatic force to do the translation, which is created by an applied voltage between the fixed part and the moveable part. These mems comb-drive actuators can be used in many scenarios, such as optical communication, biomedical engineering, wireless communication, resonators, and electromechanical filters[3,4].

In this experiment, we use photolithography tool to define the wiring. Then we use deep reactive ion etching (DRIE) to etch silicon and form free-standing structures and finally use HF to selectively etch silicon dioxide to release part of the structures combined with critical point dry techniques to prevent devices from collapsing due to stiction. We manufacture 18 comb-drive devices, each type of device with different feature dimensions that affect the performance of comb-drive.

II. Experiment

We begin our mems fabrication by depositing 150 nm thick of chromium using physical vapor deposition standard recipe with PVD-02 and PVD-04 to the 6 μm doped polycrystalline silicon wafer. The PVD process is manipulated under $3.5*10^{-6}$ Torr achieved by using roughing pump (10^{-2} torr) and diffusion pump (10^{-6} torr). We expose the coated wafer by photolithography using MA-01 Suss MA6, choosing the "ESE536MEMSlevel1" recipe to define wiring. Since there exists a gap between mask and wafer, the resolution depends on the diffraction of light through the photomask. To minimize the effect of diffraction, we expose the pattern through vacuum contact mode and make the mask as clean as possible. In the process of stripping the photoresist, we use DE-08 Jupiter II RIE for a minute under 1.2 Torr first, then we remove the rest using deionized water for 5 minutes at 60℃. The reason is that not all of the photoresist may dissolve in solvent since it has been exposed to plasmas. With oxygen plasma stripping technique, oxygen radicals and ions can decompose organic matter in the photoresist, which can be further removed by solvent. After this process, we inspect the wafer using the Zeiss M2M microscope and find that the wiring layer is well defined.

Before we do photolithography, the wafer is spin-coated with HMDS and S1813 for 45s at 3500 rpm, respectively. The HMDS is used as an adhesion promoter for photoresist[5]. Then we pattern our wafer using MA-01 Suss MA6, choosing the "ESE536MEMSlevel2" recipe. This is performed with strict alignment to level 1 pattern. After that, we conduct deep silicon etch (DRIE)

Using DE-03 STPS DRIE with "ESE 536_Deep" recipe to form moveable structures with high contrast ratio on devices. The number of cycles determines the etch depth, and this process includes 15 periods, with 600nm deep each

cycle. We then inspect the wafer using the Zeiss M2M microscope and find 18 types of comb-drive patterns, four types of z-axis cantilever beams, and six types of y-axis cantilever beams. In each device, there are 50 teeth in a comb, and eight flexing beams in a folded beam configuration.

After we have formed the moveable comb-drive structures, we use the hydrofluoric acid to remove the SiO_2 scaffolding to create free-standing silicon mechanical structures in the WB-06 HF wet bench. This process is performed for 6 minutes under well control so that not all SiO_2 is removed, and leave some SiO_2 elements to anchor structures to the substrate and maintain the mechanical properties of devices. Followed up by rinsing wafer in deionized water to remove hydrofluoric acid residual, the drying process is carried out under critical point drying using CPD-01 Tousimis. Utilizing the property of a particular solvent which it can be heated at high pressure to transform into super-critical fluid so that it will not change from liquid to vapor when expanded, this step avoids the surface tension at the liquid-vapor interface, which pulls mechanical structures toward each other as device dries. We choose liquid CO_2 for its critical point temperature is just above room temperature as well as it can mix well with many solvents. Finally, we mount the chip to pc board and wire bond contacts using BE-03 K&S Wire Bonder and test our devices.

III. THEORY

First, the energy stored in the capacitor between the fixed comb and moveable comb can be given as:

$$E = \frac{1}{2} C V^2 \tag{1}$$

Where C is the capacitance of the parallel plate capacitor, which is the capacitance between two parallel combs. V is the applied voltage. The electrostatic force can be derived by differentiating the energy stored in the two plates of the capacitor with respect to the direction of the force as:

$$F = \frac{1}{2} \frac{\partial C}{\partial x_{drive}} V^2 \tag{2}$$

As a result, the comb-drive electrostatic force can be further written by:

$$F_{electrostatic} = -\frac{\varepsilon_0 n h}{d} V^2 \tag{3}$$

Where n is the number of combs, d is the separation distance between comb to comb. ε is the vacuum permittivity. Next, we define the elastic force in the beam by first deriving the elastic strain energy, which can be written as:

$$U_{beamlet} = \frac{1}{2} \frac{Eh}{4} \left(\frac{b}{L_b} \right)^3 x^2 \tag{4}$$

Where E is the young's modulus for silicon, h is the silicon thickness, b is the beam width, and L_b is the beamlet width. The x represents the deflection of the tip of the beam. As a result, the elastic strain force of the beam can be expressed as the derivative of the strain energy with respect to the displacement of the beam, which is:

$$F_{strain} = 2Eh \left(\frac{b}{L} \right)^3 x \tag{5}$$

Then we set the sum of electrostatic force and elastic force to zero, and we can get the expression of the deflection of comb versus applied voltage as follows:

$$y = \frac{\varepsilon_0}{2E} \frac{n}{d} \left(\frac{L}{b} \right)^3 V^2 \tag{6}$$

As can be seen from the equation above, theoretically, the deflection is independent of the thickness h and varies inversely with comb-drive separation d as well as the beam width b.

Next, we derive the deflection of the cantilever beam. The mechanical force of the cantilever beam can be given by Hooke's law, which is:

$$F = kx \tag{7}$$

Where k is spring constant. The electrostatic force of the cantilever beam can be derived through the same method, which is:

$$F_E = \frac{1}{2} \frac{\varepsilon W L}{(g - x)^2} V^2 \tag{8}$$

Where L, W, and T represents the dimensional features of the beam, L is the length, W is width, and T is the thickness of the beam. ε is the permittivity of the material of the cantilever beam. The gap of the beam and wafer is represented by g.

Here we define the effective force of the cantilever beam system, which combines the electrostatic force as well as mechanical force. The sum of two components should equal to zero when the system is at equilibrium:

$$F_{eff} = -\frac{1}{2} \frac{\varepsilon W L}{(g - x)^2} V^2 + kx = 0 \tag{9}$$

Where F_{eff} is the net force applied on the cantilever beam. The spring constant can be further written as:

$$k = \frac{3EI}{L^3} = \frac{1}{4} \frac{EWT^3}{L^3} \tag{10}$$

The momentum of inertia I can be approached by simplifying cantilever as a cuboid. As a result, the deflection of the tip of the beam can be rewritten as:

$$x = \frac{1}{3}\frac{FL^3}{EI} = \frac{2\varepsilon L^4}{ET^3 g^2}V^2 \tag{11}$$

Note that this formula is valid only when deflection is small so that the angle of deflection is small. Hence, the mechanical force can be considered in the same direction as the movement of the tip of the cantilever beam. Theoretically, the deflection of the beam goes as quadratic relation as applied voltage, for another parameter is constant for a given beam system.

When testing comb-drive devices, the voltage should not be applied too high, or the beam would snap down. Snap-down occurs when:

$$\frac{\partial F_{eff}}{\partial x} = 0 \tag{12}$$

we can get the snap-down voltage as well as maximum deflection using the equation above:

$$V_p = \sqrt{\frac{8}{27}\frac{kg^3}{\varepsilon WL}} \tag{13}$$

$$x = \frac{1}{3}g \tag{14}$$

The fundamental bending frequencies can be given by the equation as follows[6]:

$$f_1 = \frac{1}{2\pi}[\frac{3.5156}{L^2}]\sqrt{\frac{EI}{\rho}} \tag{15}$$

Where ρ is given by the formula $\rho = m/L$, m is the mass of beam. Here we use the first-order bending of fixed-fixed beam vibration modes to describe the motion of the beam. The resonant frequency is simply the double of applied frequency, given by:

$$f_R = 2 \times f_{applied} \tag{16}$$

IV. Results And Discussion

Compare with SEM[8] measurements, the value of comb-drive e_3 b measured by optical microscope deviates around 2.7% to 4.2%. As for optical microscope measurement for different comb-drives, the deviation of experimental value and theoretical value ranges from 1% for e_1 comb gap, to 11.7% for e_2 comb gap. It shows that e_1, e_3, f_1, and f_3 fit the settled data well, but e_2 and e_3 present a substantial difference from the ideal feature size, which may occur due to the overexposure or the different etching degree.

The feature size is measured by Zeiss M2M Microscope and Electron Microscope. The bar shows the accuracy of the feature is measured. The scanning frequency is connected with the resolution—generally, the higher the frequency, the higher the quality of the image.

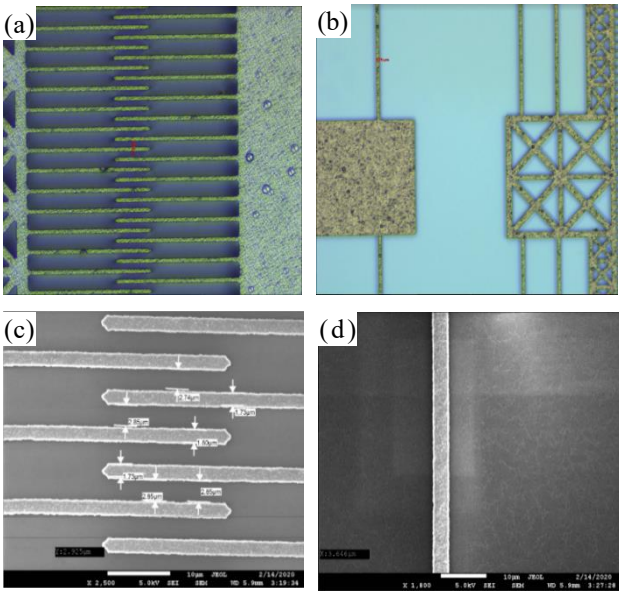

Fig. 1. Comb drive feature size measurements. (a) Optical microscope image of comb separation d. (b) Optical microscope image of beam width d. (c) SEM image of comb separation d. (d) SEM image of beam width d.

Five sets measurements, including the comb to comb separation as well as the bandwidth. The settled and measured feature size is presented to make a comparison.

TABLE I

Optical Microscope Measurement Of Comb-Drive Feature Sizes

Comb-drive	b_0/μm	d_0/μm	b/μm	d/μm
e_1	3.6	2.0	3.76	1.98
e_2	3.6	2.4	3.82	2.12
e_3	3.6	2.8	3.75	2.73
f_1	4.0	2.0	4.78	2.12
f_3	4.0	2.8	4.17	2.73

TABLE II

Optical Microscope And SEM Measurement Of E_3 Feature Size

Tools	b/μm	d/μm
SEM	3.65	2.85
Optical Microscope	3.75	2.73

The image of SEM has a higher resolution and a smaller minimum feature size than the microscope. The SEM shows more details of the surface morphology with the intensity of the brightness of the image. On the microscope image, the bandwidth and comb drive distance seem uniform, while the

SEM images show the fluctuation of the distance between two different combs.

The electrical experiment is conducted by measuring AC and DC characteristics of the cantilever. Applying potential and moved with frequency or direct current.

There are 44 connectors on the circuit board with half on the front and the other on the back. They are wire-bonded with the silicon devices on the wafer with comb drives, vertical cantilevers as well as horizontal cantilevers. The optical profilometer is using interfering effects to measure step heights and distances between structures.

For the AC measurement of cantilevers, the AC signal is applied, and the force is switching from the attractive force and 0, which will show attractive force twice for each cycle. The resonant frequency of the cantilever beams in experiments is two times of the applied frequency. Once it reaches the resonant frequency, the tip of the cantilever shows twisting morphology.

The length of the two cantilevers that measured is 300 microns and 200 microns. The theoretical value of the fundamental frequency of the 300 microns was 84.4 kHz, calculated by the equation (15) and (16). And the experiment value is 84.2 kHz.

To calculate the fundamental theoretical frequency, the relationship of cantilevers with different lengths are as follows:

$$f_b = \frac{L_a^2}{L_b} \times f_a \qquad (17)$$

In this equation, L_a is 300 microns, and L_b is 200 microns. The theoretical frequency is 121.8 kHz. The experimental frequency is 118.4 kHz.

The discrepancy is due to the systematic error as well as the artificial error. The precision of the instrument influences the testing result. And the resonance phenomenon was artificially measured, which leads to the discrepancy of the real frequency and the recorded ones.

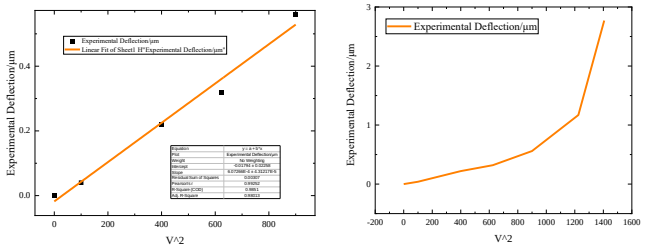

Fig. 2. Experimental deflection data linear fitting of V^2 ($V \leqslant 30V$) and plot of experimental data vs. V^2.

For the vertical cantilever, the positive voltage was applied to the cantilever and negative voltage on the substrate. According to the plot of d vs. V, it is obvious to see a significant increase at the voltage of 30 V, from which the slope shows a noticeable change. And at the voltage of 37.5 V, the deflection had been reached to the height of the cantilever. That is where the cantilever snapped down to the substrate.

F_{eff} is composed of electrostatic force and mechanical force. The snap-down occurs when dF/dx equals to 0, where x=1/3g. We can use this equation to calculate theoretical snap-down voltage, for which the deflection is 0.92 microns.

Accordingly, the deflection of cantilever is linear with the square of the voltage. From the result of the linear fitting, before the voltage increased to 30 V, it shows a good approximation of linear relationship with V^2. It can be concluded that the electrostatic and elastic force is in equilibrium. It can be deducted that the snapped down occurred after 35 V, for the deflection kept increasing after the voltage applying. Then the snap-down deflection in practical is larger than 1.17 microns, where the force of the electrostatic overpassed the elastic force of the beam, which makes the cantilever destabilized.

Hence, the experimental discrepancy takes over 27.2% of the theoretical value, which is due to the cantilevers were not lined horizontally. They have a higher step at the tip, which requires additional voltage to bend into the horizontal level.

The deflection and voltage were measured by Zygo. First, we choose the same horizontal line on a comb and apply voltage on the comb drive. Then we use orange and blue light to decide the baseline. Next, we put these two lines on the bottom to the step height to do X_{dst} measurement. Write down the X distance and the voltage.

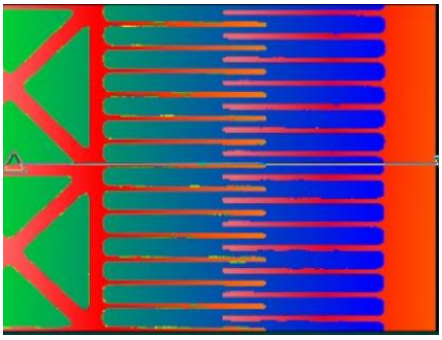

Fig. 3. Zygo image of comb separation measurement at 0 V

First, we calculate the theoretical deflection of comb drives a_2 (b=2, d=2.4) and d_3 (b=3.2, d=2.8) by equation (6).

Then the ideal deflection and experimental vs. V^2 are plotted. The deflection of the comb drive was calculated by

the initial distance minus the distance after the linear fitting result of the statics is also presented on the graph.

The deflection is increasing as the voltage adding with time, whether in theory or practice. And the attractive force which is electrostatically generated by the potential difference.

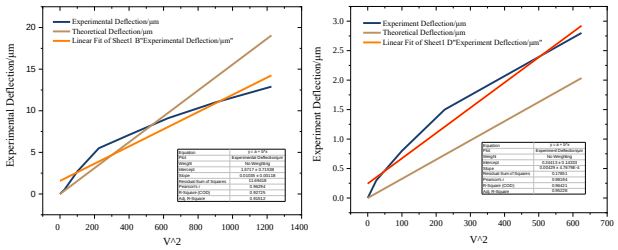

Fig. 4. Experimental deflection of comb drives a_2 (left) and d_3 (right) vs. V^2 and linear fitting of the experimental data.

For comb drive a_2, the linear fitting of the statistics presents the slop of 0.01035±0.00118, which is lower than the theoretical linear slope of 0.01556. While for the b_3, the experimental statistics show better linear fitting with higher R-value. The slope of the linear fitting of experimental results is 0.00429±0.00048. And the slope of the theoretical slope is 0.00326. The experiment result can fit the theoretical tendency as voltage increases.

Compared with the Thursday and Friday process and results, it shows the adjustment of the processing time and method can efficiently avoid some defects of the sample. After the process of HF etching, DI water rinsing, and critical point drying, the microscope of the surface shows evident moisture and residue. Which can be the first cause of the snapped down. The HF etching time was decreased by 1 min to eliminate the moisture, which can reduce the undercut that might hold the HF. Besides, the water rinsing time was also increased by 3 min to increase the resolving of HF into the solvent. According to the result, there is no residue but some moisture after CPD[7]. Therefore, the CPD process was changed like the O-rings, and some of the methanol was removed to leave more space for CO_2 and methanol to mix. And the flow increases to two times the original time length to make the drying more complete. As a result, there was no residue as well as moisture. There was no snapped down, and the cantilevers worked well. However, the comb drive didn't move. To solve the problem and make sure of the causes, we should control the variables. To set different times of etching, rinsing, and drying separately. Then inspect the surface and make an electrical measurement of the comb drives to see if it can work.

V. Conclusions

The nanofabrication procedures of comb-drive, horizontal, and vertical cantilevers were conducted. By changing HF etching time, water rinsing time, and improving the degree of MeOH and carbon dioxide mixing, the devices can become free-standing. However, it is necessary to overcome the problem that combs did not move under the application of voltage. The cantilever could present deflection, which shows electrical connection works well. Therefore, the etching, rinsing, and CPD processing still needs to be improved. According to the measurement, the data of feature sizes of comb drives, deflection, and resonant frequency fits the theoretical data. But the device we fabricated still far from the ideal situations, for the height of the combs is not always constant, and the measure of size and signal has obvious system limits and artificial errors. The next experiment is supposed to focus on measuring errors by increasing the measuring times and controlling the step of applying a voltage to be not too large.

References

[1] M. Olfatnia, S. Sood, J. J. Gorman and S. Awtar, "Large Stroke Electrostatic Comb-Drive Actuators Enabled by a Novel Flexure Mechanism," in Journal of Microelectromechanical Systems, vol. 22, no. 2, pp. 483-494, April 2013.

[2] Rosing, R. & Reichenbach, Ralf & Richardson, Andrew. (2002). Generation of component level fault models for MEMS. Microelectronics Journal. 33. 861-868. 10.1016/S0026-2692(02)00097-6.

[3] Gupta, S., Pahwa, T., Narwal, R., Prasad, B., & Kumar, D. (2012). Optimizing the Performance of MEMS Electrostatic Comb-drive Actuator with Different Flexure Springs.

[4] Legtenberg, R., Groeneveld, A. W., & Elwenspoek, M. C. (1996). Comb-drive actuators for large displacements. *Journal of micromechanics and microengineering*, *6*(6), 320-329. https://doi.org/10.1088/0960-1317/6/3/004

[5] Cornell NanoScale Science & Technology Facility. "CNF - Photolithography Resist Processes and Capabilities". Retrieved 2008-01-29

[6] Chollet, F., & Liu, H. (2006). A not so short Introduction to Micro Electromechanical Systems.

[7] Bray, Douglas. (2008). Critical Point Drying of Biological Specimens for Scanning Electron Microscopy. 10.1385/1-59259-030-6:235.

[8] Goldstein, J. I., Newbury, D. E., Michael, J. R., Ritchie, N. W., Scott, J. H. J., & Joy, D. C. (2017). Scanning electron microscopy and X-ray microanalysis. Springer.

AUTHOR INFO

Shenshen Wan, received Bachelor of Science in Polymer Materials from Sichuan University, 2015.

Minzhong Gao, received Bachelor of Science in Engineering degree in Aerospace Engineering from Beijing Institute of Technology, 2015.

ATTACH ANCILLARY DATA

A. *Traveler*

ESE 536 MEMS Page 1 of 3

Date	Operation	Tool	Comment	Signoff
	Thermal Anneal, 30 min, 1050° C, N2 atmosphere	CVD-02 D Anneal	TA preparation	
	Wafer Start, Blowoff with N2, label carrier		TA preparation	
	Etch in HF to remove SiO2 protective coating and surface oxides, rinse and dry	WB-03 HF Bench	TA preparation	
	Evaporate Cr, 150 nm, standard recipe, Kapton tape wafers to large chuck. Start process at 3.5E-6 Torr	PVD-02 and PVD-04	E-beam thermal evaporation Roughing pump+diffusion pump	
	Spin coat S1813, 3500 rpm 45s, softbake 60 s, 115° C	SPN-01, SPN-05	Press the pedal as soon as S1813 is added to the wafer	
	Expose, MA6, "ESE536MEMSlevel 1", 70 m J/cm2 "Metal" Mask	MA-01 Suss MA6	Use the indicator on the stage to locate the wafer into correct position	
	Develop, MA319 60s, manual agitation, rinse 2x, dry	wet bench	Manual agitation to boost the reaction process	
	Inspect, Zeiss microscope	Zeiss M2M	Select the highest practical magnification	
	Wet etch Cr, 1020AC, 200s, rinse 2x	wet bench	Manual agitation to boost the reaction process	
	Strip resist, Oxygen Plasma, 1 min, 1.2Tor	DE-08 Jupiter II RIE	Solvent stripping is not enough Oxygen radicals decompose organic matter	
	Strip resist, 1165, 60° C, 5 min, DI water rinse, spin rinse dry	wet bench	Blow nitrogen perpendicular to the edge of wafer to remove residual moisture	
	Inspect, Zeiss microscope	Zeiss M2M	Select the highest practical magnification	
	Dehydation bake wafer, 115° C 3 minutes	hotplate	To get rid of moisture, which makes it easier for HMDS to coat	

ESE 536 MEMS Page 2 of 3

Date	Operation	Tool	Comment	Signoff
	Spincoat HMDS, 3500 rpm, 45 s	spin coater	Press the pedal as soon as HMDS is added to the wafer, or the HMDS will self-assemble	
	Spin coat S1813, 3500 rpm, 45 s, softbake 60 s, 115° C	spin coater	Let the wafer cool down before next step	
	Expose, MA6, 80 mJ/cm2, "ESE536MEMSLevel 2" recipe, Si Etch Mask	MA-01 MA6	Make sure the mask is aligned correctly with respect to layer 1	
	Develop, MF-319, 60 s, maual agitation, rinse 2x	wet bench	Manual agitation to boost the reaction process	
	Inspect, Zeiss Microscope	Zeiss M2M	Select the highest practical magnification	
	Si Etch, ESE 536_Deep recipe (600 nm/cycle) 15 cycles	DE-03, STPS DRIE	Each cycle is a little bit more than 600 nm to ensure the depth of Si etch	
	Inspect, Zeiss microscope	Zeiss M2M	Select the highest practical magnification	
	Strip Resist, O2 plasma 3 min, 1.5 torr, 50W	DE-08 Jupiter II RIE	Harsh plasma exposed resist becomes hard to remove. O_2 plasma to remove thin residue	
	Strip Resist, 1165 5 min 65° C, rinse 2x	wet bench	Strip remaining resist in hot NMP	
	Inspect	Zeiss M2M	Select the highest practical magnification	
	Measure step height	MET-01/ MET-02	Avoid the boundary of the measurement where large noise exists	
	Cleave wafer, hand cleave w diamond scribe, 2 chips, N2 blowoff		The wafer will be cleaved follow the lattice growth direction theoretically	
	HF release, HF etch 6 min, DI water rinse 2 min, bath	WB-06 HF wet bench	Put on HF gowning suit to perform this step. Let the DI water fully heated before putting the chip	

ESE 536 MEMS Page 3 of 3

Date	Operation	Tool	Comment	Signoff
	MeOH rinse 4x	solvent bench	Methanol can mix with water and CO2, replace with methanol as intermediary	
	Critical Point Dry	CPD-01 Tousimis	Avoid pattern collapse due to surface tension at liquid-vapor interface	
	Inspect, optical microscope	Zeiss M2M	Select the highest practical magnification	
	Mount to pc board with silver appoxey		TA preparation	
	Wirebond contacts	BE-03 K&S Wire Bonder	TA preparation	

B. *Comb-drive displacement vs. voltage relationship*

First, we derive the elastic strain energy of the folded beam of comb-drive, which can be described as follows:

$$F_{beamlet} = ky_b = \frac{3IE}{L_b^3} y_b \tag{18}$$

$$I = \frac{hb^3}{12} \tag{19}$$

$F_{beamlet}$ is the force exerts on the beam, and I is the momentum of inertia of the beam. The energy can be described as the integral of the force over the deflection of the beam:

$$U_{beamlet} = \int_0^{y_b} F_{beamlet} dy \tag{20}$$

Which reduces to:

$$U_{beamlet} = \int_0^{y_b} \frac{3IE}{L_b^3} y_b dy = \frac{Eh}{8} (\frac{b}{L_b})^3 {y_b}^2 \tag{21}$$

Elastic strain force is the derivative of the strain energy with respect to the total displacement, y:

$$F_{strain} = \frac{dU_{beamlet}}{dy} \tag{22}$$

Which reduces to:

$$F_{strain} = 8\frac{Eh}{8} (\frac{b}{L_b})^3 \frac{dy^2}{dy} = 2Eh(\frac{b}{L})^3 y \tag{23}$$

Suppose the two plates of interdigitated structures are parallel, the electrostatic force of come-drive can be given as:

$$C = \frac{\varepsilon A}{d} = \frac{\varepsilon xh}{d} \tag{24}$$

The electrostatic force can be derived by differentiating the energy stored with respect to x as:

$$F = \frac{1}{2} \frac{\partial C}{\partial x_{drive}} V^2 \tag{25}$$

Which reduces to:

$$F_{electrostatic} = -\frac{\varepsilon_0 nh}{d} V^2 \tag{26}$$

Next, we sum the electrostatic force and elastic force as follows:

$$2Eh(\frac{b}{L})^3 y - \frac{\varepsilon_0 nh}{d} V^2 = 0 \quad (27)$$

Solving for y, we can get the expression of the deflection of comb versus applied voltage as follows:

$$y = \frac{\varepsilon_0}{2E} \frac{n}{d} \left(\frac{L}{b} \right)^3 V^2 \quad (28)$$

C. *Displacement And Frequency Response Raw Data*

TABLE III

OPTICAL MICROSOPE MEASUREMENT OF COMB-DRIVE A_2

V^2	Experimental Deflection/μm	Theoretical Deflection/μm
0	0	0
25	0.5	0.388916
100	2.7	1.555664
225	5.5	3.500244
400	7.1	6.222656
625	9.1	9.722901
900	11	14.00098
1225	12.9	19.05689

TABLE IV

OPTICAL MICROSOPE MEASUREMENT OF COMB-DRIVE D_3

V^2	Experimental Deflection/μm	Theoretical Deflection/μm
0	0	0
25	0.3	0.08139
100	0.8	0.32554
225	1.5	0.73247
625	2.8	2.03465

TABLE V

DC MEASUREMENT OF VERTICAL CANTILEVER BEAM

V^2	Experimental Deflection/μm
0	0
100	0.04
400	0.22
625	0.32
900	0.56
1225	1.17
1406.25	2.77

TABLE VI

AC MEASUREMENT OF VERTICAL CANTILEVER BEAM

Length/μm	Experimental Frequency/kHz	Ideal Frequency/kHz
200	118.4	121.8
300	84.4	84.2

D. *Mini project*

For the comb-drive device under the same exposure gap, the simulation shows that the resolution of comb-drive increases with the threshold rising from 0.1 to a particular value of threshold where the resolution reaches a peak. Then the resolution decreases with the threshold continues increasing to the maximum value. This variation concerning the change of threshold turns out to be the same for both of the exposure gaps. However, the peak value of the threshold where resolution reaches the maximum varies for these two samples. In the exposure gap of 15 microns, the peak value approximately equals 0.5, where for 6 microns sample, the peak value is around 0.4.

Using images collected from the optical microscope, we can find that under 6 microns exposure gap, the resolution of comb-drive devices is higher than resolution under 15 microns of the exposure gap. The decreasing resolution is due to the increase in the exposure gap, which leads to higher Fresnel diffraction. This observation holds the same for simulations. Under the same ratio of dose to clear resist and provided dose, the resolution of interdigitated combs decreases with the exposure gap increasing for six pairs of simulations.